A random matrix/transition state theory for the probability distribution of state-specific unimolecular decay rates: Generalization to include total angular momentum conservation and other dynamical symmetries

Rigoberto Hernandez, William H. Miller, and C. Bradley Moore
Department of Chemistry, University of California, and Chemical Sciences Division, Lawrence Berkeley Laboratory, Berkeley, California 94720

William F. Polik
Department of Chemistry, Hope College, Holland, Michigan 49423

(Received 9 March 1993; accepted 2 April 1993)

A previously developed random matrix/transition state theory (RM/TST) model for the probability distribution of state-specific unimolecular decay rates has been generalized to incorporate total angular momentum conservation and other dynamical symmetries. The model is made into a predictive theory by using a semiclassical method to determine the transmission probabilities of a nonseparable rovibrational Hamiltonian at the transition state. The overall theory gives a good description of the state-specific rates for the $D_2CO \rightarrow D_2 + CO$ unimolecular decay; in particular, it describes the dependence of the distribution of rates on total angular momentum J. Comparison of the experimental values with results of the RM/TST theory suggests that there is mixing among the rovibrational states.

I. INTRODUCTION

In a recent series of experiments, Polik *et al.*[1] determined the unimolecular reaction rates for the decomposition of formaldehyde in its ground electronic state

$$D_2CO \rightarrow D_2 + CO \qquad (1.1)$$

for *individual quantum* (i.e., rovibrational) *states* of the reactant molecule. Although standard statistical theory [i.e., Rice–Ramsperger–Kassel–Marcus (RRKM), microcanonical transition state theory, etc.] provides a good description of the rate as a function of the energy of the molecule *on the average*, the decay rates of individual quantum states with energies in a given energy interval show significant fluctuations about the average rate for that energy (interval). Figure 1 shows a schematic depiction of this situation.

Miller and co-workers[2,3] showed how to combine random matrix theory with transition state theory to provide a theoretical model for describing the distribution of state-specific decay rates about their average. The essential assumptions of this random matrix/transition state theory (RM/TST) model are that the states be nonoverlapping and *strongly mixed*. The first assumption is clearly satisfied if the experiments resolve individual quantum states. By *strongly mixed*, we mean that the system behaves like the Gaussian orthogonal ensemble of random matrix theory.[4] Physically, this latter requirement is equivalent to the assumption that the expansion coefficients (in some generic basis) of the eigenstates in a given energy interval all behave as independent random variables. The good agreement of various spectral measures between the experimental results and predictions of the Gaussian orthogonal ensemble indicates that the eigenstates of D_2CO are indeed well described as *strongly mixed*.[3]

The purpose of this paper is twofold—first to show how total angular momentum conservation (and other dynamical symmetries) can be incorporated into the RM/TST model for the probability distribution of state-specific decay rates, and second to show how a recently developed semiclassical transition state theory can be utilized to make it a predictive theory. Section II A first summarizes the essentials of the RM/TST model developed previously and the semiclassical transition state theory for a general anharmonic rovibrational transition state is described in Sec. II B, with specific application to the RM/TST model. Section II C then shows how this RM/TST theory is modified to account for dynamical symmetries. As an aside, Appendix A presents an expression for the microcanonical quantum survival probability resulting from the distribution of decay rates given by the RM/TST theory of Sec. II.

Application of the theory to reaction (1.1) is made in Sec. III, where the primary new results are the dependence of the probability distributions on total angular momentum J. Since the results given by the RM/TST theory depend rather sensitively on which degrees of freedom one assumes are strongly mixed and which are approximately conserved, the calculations were carried out with various assumptions to see which gave the best agreement with experiment. Specifically, RM/TST theory is used to obtain the probability distribution for the individual J states of D_2CO assuming conservation of total angular momentum J, conservation of the angular momentum projection onto a space-fixed axis M, and either (a) no additional conserved quantities; (b) conservation of C_s symmetry; or (c) conservation of C_s symmetry and the absolute value of the angular momentum projection onto a body-fixed axis $|K|$. In addition, the distribution for all the decay rates is obtained under these conditions. Comparison to the experimental distributions indicates that case (a) can account for the unimolecular reaction dynamics at high electric field. However, it is possible that J mixing can also provide similar agreement.

 0021-9606/93/99(2)/950/13/$6.00

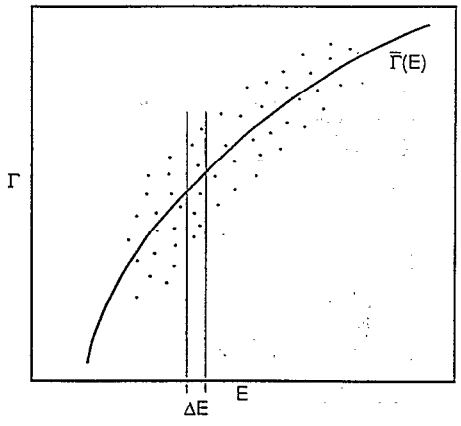

FIG. 1. Unimolecular decay rate vs energy. The points indicate the decay rates and energies for individual quantum states of the reactant molecule. $\bar{\Gamma}(E)$ is the *average rate* averaged over all the states in a given narrow energy interval δE.

II. THEORY

A. Summary of basic RM/TST model

A system undergoing unimolecular dissociation can, in general, be described by an effective Hamiltonian matrix[5,6] of the form

$$\mathscr{H}^{\text{eff}}_{m,m'}=\mathscr{H}_{m,m'}-\frac{i}{2}\Gamma_{m,m'}, \tag{2.1}$$

where $\{|m\rangle\}$ is some bound-state ($\mathbf{L}^2$) basis which spans the (Hilbert) space of the reactant molecule. The real symmetric matrix $\mathscr{H}_{m,m'}$ describes coupling (anharmonic, Coriolis, etc.) in the reactant molecule. The decay rate matrix $\Gamma_{m,m'}$ describes the coupling of the bound states $\{|n\rangle\}$ to a continuum of unspecified scattering states of the dissociated molecule. The complex eigenvalues of $\mathscr{H}^{\text{eff}}$, $\{E_j-\frac{i}{2}\Gamma_j\}$, give the energies $\{E_j\}$ and decay rates $\{\Gamma_j\}$ of the individual quantum (metastable) states of the reactant molecule provided they are nonoverlapping, i.e.,

$$\Gamma_j<|E_j-E_{j'}|. \tag{2.2}$$

(Alternatively, $\{E_j\}$ and $\{\Gamma_j\}$ are the positions and widths of scattering resonances between bimolecular collisions of the fragment molecules.) In light of Eq. (2.2), it is reasonable to treat the imaginary part of $\mathscr{H}^{\text{eff}}$ by first order perturbation theory. The "zeroth order" eigenstates

$$|\Psi_j\rangle=\sum_m |m\rangle c_{m,j} \tag{2.3}$$

are thus the eigenvectors of the real Hamiltonian matrix $\mathscr{H}$ and the imaginary parts of the eigenvalues are given (within first order perturbation theory) by

$$\Gamma_j\equiv\langle\Psi_j|\Gamma|\Psi_j\rangle=\sum_{m,m'} c_{m,j}\Gamma_{m,m'}c_{m',j}=\mathbf{c}_j^T\cdot\boldsymbol{\Gamma}\cdot\mathbf{c}_j. \tag{2.4}$$

The unimolecular decay rate for a state characterized by eigenvector $\mathbf{c}$ is therefore $\Gamma(\mathbf{c})=\mathbf{c}^T\cdot\boldsymbol{\Gamma}\cdot\mathbf{c}$.

One next assumes that the eigenstates of $\mathscr{H}$ are *strongly mixed*, i.e., that the dynamics of the (highly excited) reactant molecule are chaotic, ergodic, etc. This corresponds to assuming that the statistics of the eigenstates within a given narrow energy interval are equivalent to sampling over all states consistent with normalization $\mathbf{c}^T\cdot\mathbf{c}=1$. Physically, this uniform sampling will involve a random mixture of only a finite number of basis states since random coupling of an infinite basis would entail the loss of energy information. Thus the "zeroth order state" reduces to the generic form

$$|\Psi_j\rangle=\sum_{m=1}^{f}|m\rangle c_{m,j}, \tag{2.5}$$

where f is the effective number of *strongly mixed* states in a generic basis. (Appendix B discusses more fully the physical significance of the parameter f.) As in random matrix theory, the normalization requirement on this f-dimensional state vector $\mathbf{c}$ is approximated by a product of Gaussian distributions, an approximation which improves with increasing f. The probability distribution of unimolecular decay rates is then given by

$$P(\Gamma)=\int_{-\infty}^{\infty}\cdots\int_{-\infty}^{\infty}dc_1\cdots dc_f\,P_f(\mathbf{c})\delta(\Gamma-\mathbf{c}^T\cdot\boldsymbol{\Gamma}\cdot\mathbf{c}), \tag{2.6}$$

where the probability distribution of the expansion coefficient is

$$P_f(\mathbf{c})=\prod_{j=1}^{f}\sqrt{\frac{f}{2\pi}}e^{-fc_j^2/2}. \tag{2.7}$$

Introducing the integral form of Dirac's δ function $\delta(z)=(2\pi)^{-1}\int_{-\infty}^{\infty}e^{izt}dt$, the integrals in Eq. (2.6) can be evaluated to give

$$P(\Gamma)=(2\pi)^{-1}\int_{-\infty}^{\infty}dt\,e^{i\Gamma t}D'(t)^{-1/2}, \tag{2.8a}$$

where

$$D'(t)=\det(1+2it\boldsymbol{\Gamma}/f)=\prod_{j=1}^{n}(1+2it\gamma_j/f), \tag{2.8b}$$

and $\{\gamma_j\}$ are the n nonzero eigenvalues of the $\boldsymbol{\Gamma}$ matrix. (Note that, in general $n\ll f$, *vis a vis* most of these eigenvalues are zero.)

Using brackets $\langle\cdot\rangle$ to denote an average with respect to the probability distribution, the average rate is given by

$$\bar{\Gamma}\equiv\langle\Gamma\rangle=\frac{1}{f}\sum_{j=1}^{n}\gamma_j=\frac{1}{f}\operatorname{Tr}(\boldsymbol{\Gamma}). \tag{2.9}$$

This determines the effective number of mixed states as

$$f=\frac{\operatorname{Tr}(\boldsymbol{\Gamma})}{\bar{\Gamma}}. \tag{2.10}$$

Similarly, the variance of the distribution is

$$(\langle\Gamma^2\rangle-\langle\Gamma\rangle^2)=\left(\frac{2}{f^2}\sum_{j=1}^{n}\gamma_j^2\right)=\frac{2}{f^2}\operatorname{Tr}(\boldsymbol{\Gamma}^2). \tag{2.11}$$

These last two results can be combined to obtain the so-called effective number of channels with respect to the Γ matrix

$$\nu_{\text{eff}} \equiv \frac{2\langle\Gamma\rangle^2}{\langle\Gamma^2\rangle - \langle\Gamma\rangle^2} = \frac{\text{Tr}(\Gamma)^2}{\text{Tr}(\Gamma^2)}. \tag{2.12}$$

Note that this provides an analytic value of ν_{eff} if the eigenvalues of Γ are known.

It is useful to define the dimensionless *reduced probability distribution* in terms of $P(\Gamma)$ as

$$p(x) \equiv \bar{\Gamma} P(\bar{\Gamma} x), \tag{2.13a}$$

where $x = \Gamma/\bar{\Gamma}$ is the decay rate in units of the average rate. From Eqs. (2.8) and (2.9), one sees that

$$p(x) = (2\pi)^{-1} \int_{-\infty}^{\infty} dt\, e^{ixt} D(t)^{-1/2}, \tag{2.13b}$$

where

$$D(t) = \det[\mathbf{1} + 2it\Gamma/\text{Tr}(\Gamma)] = \prod_{j=1}^{n} [1 + 2it\gamma_j/\text{Tr}(\Gamma)]. \tag{2.13c}$$

If there are exactly n equal nonzero eigenvalues, i.e., $\gamma_j = \gamma$ for $j \leqslant n$, Eq. (2.13) reduces to a χ^2 distribution with n degrees of freedom, and this has been the traditional model used to describe fluctuations in unimolecular decay rates.[7,8] In this case, $\nu_{\text{eff}} = n$. If there are two nonzero and nonequal eigenvalues of arbitrary degeneracy, the integral is of the form of a confluent hypergeometric function;[2] this form exhibits a more general type of behavior than that observed with the χ^2 distributions.[2] In the most general case, one can obtain the distribution from Eq. (2.13) by numerical integration provided, of course, that one has the eigenvalues $\{\gamma_j\}$ of Γ. Note that these expressions are written as Fourier transforms in order to suggest the use of a fast Fourier transform (FFT) numerical procedure for their evaluation. If instead, a direct integration is desired, then these expressions can be written in a manifestly real form; see Eqs. (3.1) and (3.2) in Ref. 2.

B. Eigenvalues of the decay rate matrix via semiclassical transition state theory

In order to convert the distribution described in the previous subsection into a predictive formula, one needs to evaluate the eigenvalues of the decay rate matrix $\{\gamma_j\}$ up to an overall multiplicative factor. In Ref. 2, an adiabatic TST was used to approximately obtain the γ_j's; here we present a more rigorous theoretical procedure to determine them. Previously, it was argued that the eigenvalues of Γ can be obtained by a vibrationally adiabatic approximation[9] within a reaction path Hamiltonian formalism.[10] The eigenvalues were shown to be proportional to the transmission probabilities $P_{\mathbf{n}}$ through the various states $\mathbf{n}$ of the activated complex, i.e.,

$$\gamma_j = \epsilon P_{\mathbf{n}}, \tag{2.14}$$

where j is the collective index $\mathbf{n}$, and ϵ is a constant of proportionality. (As an aside, Appendix B presents a discussion relating ϵ to the RM/TST parameter f.) This suggests that an even better approximation for the eigenvalues of Γ can be obtained by constructing "good action-angle variables"[11] locally about the saddle point (i.e., transition state) of the potential energy surface. An expansion of the potential to successive orders introduces anharmonicity *vis a vis* reaction path curvature. Thus while the system is assumed to be locally integrable, there is no adiabatic assumption involved. The details of this method have already been presented for the transmission probabilities of D_2CO for total angular momentum $J=0$.[12] Here we outline this semiclassical method and include nonzero angular momentum.

Provided anharmonic and Coriolis couplings are not too strong, there will in general exist a local set of "good" classical action variables $\{I_k; k=1,...,F\}$ about a saddle point on the potential energy surface just as there does about a minimum. The essential difference though is that one of the action variables associated with the saddle point is *imaginary*, $I_F = -i\theta/\pi$, in terms of which the semiclassical transmission probability is given by

$$P = (1 + e^{2\theta})^{-1}. \tag{2.15}$$

The semiclassical procedure is therefore first to express the classical Hamiltonian as a function of the "good" actions $\mathscr{H}(\{I_k\})$, then to quantize the real actions by the usual semiclassical condition, e.g.,

$$I_k = (n_k + \tfrac{1}{2}), \quad k = 1,...,F-1, \tag{2.16}$$

and finally to determine θ as a function of the total energy E and the locally conserved quantum numbers $\{n_k; k = 1,...,F-1\}$ by solving the equation

$$\mathscr{H}\left(n_1 + \frac{1}{2}, n_2 + \frac{1}{2}, ..., n_{F-1} + \frac{1}{2}, -\frac{i}{\pi}\theta\right) = E \tag{2.17}$$

for $\theta(E,\mathbf{n})$. {We refer to θ as the generalized barrier penetration integral because it is given by the well-known integral

$$\theta = \int_{\text{barrier}} dq \sqrt{2m[V(q) - E]} \tag{2.18}$$

for a one-dimensional barrier.} With $\theta(E,\mathbf{n})$ so determined, the transmission probability for energy E and state $\mathbf{n}$ of the activated complex is

$$P_{\mathbf{n}}(E) = (1 + e^{2\theta(E,\mathbf{n})})^{-1}. \tag{2.19}$$

Angular momentum is included in the above formulas simply by noting that the classical Hamiltonian will, in general, also be a function of its magnitude J and its projection onto a body-fixed axis K. (If the molecule is not a symmetric top, K is not a good quantum number, but may still be used to label the rotational energy levels. In either case, there will be $F = 3N-6$ vibrational quantum numbers for an N atom nonlinear system.) Equation (2.17) is thus changed to read

$$\mathscr{H}\left(n_1+\frac{1}{2},n_2+\frac{1}{2},\ldots,n_{F-1}+\frac{1}{2},-\frac{i}{\pi}\theta,J,K\right)=E, \tag{2.20}$$

which determines $\theta(E,\mathbf{n},J,K)$ and thereby the transmission probability is

$$P_{\mathbf{n},J,K}(E)=(1+e^{2\theta(\mathbf{n},J,K;E)})^{-1}. \tag{2.21}$$

Moreover, the Hamiltonian may be obtained quantum mechanically and use of the correspondence

$$\theta(\mathbf{n},J,K;E)=\frac{\pi}{i}\left[n_F(\mathbf{n},J,K;E)+\frac{1}{2}\right] \tag{2.22}$$

leads to a Hamiltonian of the form in Eq. (2.20) which can then be inverted to obtain $P_{\mathbf{n},J,K}(E)$.

Determining the Hamiltonian as a function of the good action variables, however, requires an analytic solution of the classical equations of motion and is thus not in general possible. It can be accomplished to a useful level of approximation though by including anharmonicity, Coriolis coupling, etc., *perturbatively* in essentially the same way they are handled in determining rovibrational energy levels of a stable molecule (i.e., about a minimum on the potential energy surface). Therefore the Hamiltonian is expanded at the transition state and only those terms which contribute to the second order eigenvalues are retained (i.e., the vibrational terms up to quartic order with respect to the mass weighted normal coordinates Q_k of the transition state, the rigid rotor terms, and the rovibrational coupling terms arising from the Coriolis interaction)

$$\mathscr{H}=V_0+\frac{1}{2}\sum_k^F\left(-\frac{\partial^2}{\partial Q^2}+\omega_k^2Q_k^2\right)+\frac{1}{6}\sum_{klm}^F f_{klm}Q_kQ_lQ_m$$
$$+\frac{1}{24}\sum_{klmn}^F f_{klmn}Q_kQ_lQ_mQ_n+\sum_\beta B_\beta J_\beta^2$$
$$-2\sum_{k,l}^F Q_kP_l\sum_\beta B_\beta\zeta_{k,l}^\beta J_\beta, \tag{2.23}$$

where V_0 is the potential energy at the saddle point, the sums over lower case letters are unrestricted sums over the F vibrational modes, and the sums over Greek letters are sums over the rotational axes. The difference from the standard rovibrational expansion[13] is that at zeroth order, the potential along the reaction coordinate (mode F) is a harmonic barrier *vis a vis* the frequency ω_F is imaginary

$$\omega_F=i|\omega_F|\equiv i\bar{\omega}_F. \tag{2.24}$$

Using second order Van Vleck perturbation theory,[13] the Hamiltonian in Eq. (2.23) is given in terms of the local good vibrational quantum numbers (or action variables $I_k=n_k+\frac{1}{2}$) by

$$E=V_0+\bar{E}_0+\sum_k^F\omega_k\left(n_k+\frac{1}{2}\right)+\sum_{k\le k'}^F x_{kk'}\left(n_k+\frac{1}{2}\right)\left(n_{k'}+\frac{1}{2}\right)$$
$$+\sum_\beta\left[B_\beta-\sum_k\alpha_k^\beta\left(n_k+\frac{1}{2}\right)\right]J_\beta^2. \tag{2.25}$$

(If the system is truly a symmetric top, then there will be at least one degenerate vibration; the treatment is then analogous to that of a linear molecule.[14]) The zeroth order constant energy correction[15] accounting for the reaction coordinate is

$$\bar{E}_0=\frac{1}{64}\sum_k^{F-1}\frac{f_{kkkk}}{\omega_k^2}-\frac{7}{576}\sum_k^{F-1}\frac{f_{kkk}^2}{\omega_k^4}+\frac{3}{64}\sum_{k\neq l}^{F-1}\frac{f_{kll}^2}{(4\omega_l^2-\omega_k^2)\omega_l^2}-\frac{1}{4}\sum_{k<l<m}^{F-1}\frac{f_{klm}^2}{[(\omega_k+\omega_l)^2-\omega_m^2][(\omega_k-\omega_l)^2-\omega_m^2]}$$
$$-\frac{1}{64}\frac{f_{FFFF}}{\bar{\omega}_F^2}-\frac{7}{576}\frac{f_{FFF}^2}{\bar{\omega}_F^4}+\frac{3}{64}\sum_k^{F-1}\frac{f_{kFF}^2}{(4\bar{\omega}_F^2+\omega_k^2)\bar{\omega}_F^2}+\frac{3}{64}\sum_k^{F-1}\frac{f_{kkF}^2}{(4\omega_k^2+\bar{\omega}_F^2)\omega_k^2}$$
$$-\frac{1}{4}\sum_{k<l}^{F-1}\frac{f_{klF}^2}{[(\omega_k+\omega_l)^2+\bar{\omega}_F^2][(\omega_k-\omega_l)^2+\bar{\omega}_F^2]}-\frac{\hbar}{16\pi c}\left(\frac{1}{I_{xx}}+\frac{1}{I_{yy}}+\frac{3}{I_{zz}}\right), \tag{2.26}$$

where $I_{\alpha\beta}$ is the moment of inertia tensor. Explicit expressions for the anharmonic constants x's in terms of the force constants f's are given in Ref. 12. There it is noted that the anharmonic constants coupling the reaction coordinate to the perpendicular coordinates are imaginary, i.e.,

$$x_{kF}\equiv -i\bar{x}_{kF}, \tag{2.27}$$

with $\bar{x}_{kF}$ strictly real for $k\neq F$. The rotational constant for mode F is also imaginary

$$\alpha_F^\beta=i\bar{\alpha}_F^\beta, \tag{2.28}$$

and modification of the standard rovibrational expression[13] yields the real quantity

$$\bar{\alpha}_F^\beta=\left(\frac{2B_\beta^2}{\bar{\omega}_F}\right)\left\{\sum_\gamma\left[\frac{3(a_F^{\beta\gamma})^2}{4I_{\gamma\gamma}}\right]-\sum_l^{F-1}(\zeta_{Fl}^\beta)^2\left(\frac{\omega_l^2-3\bar{\omega}_F^2}{\omega_l^2+\bar{\omega}_F^2}\right)\right.$$
$$\left.-\pi\left(\frac{c}{\hbar}\right)^{1/2}\left(\frac{f_{FFF}a_F^{\beta\beta}}{\bar{\omega}_F^2}-\sum_l^{F-1}\frac{f_{FFl}a_l^{\beta\beta}}{\omega_l^2}\right)\right\}, \tag{2.29}$$

where $\mathbf{a}^{\beta\gamma}$ is the first derivative of the moment of inertia tensor $I_{\beta\gamma}$ with respect to the normal mode coordinates. The remaining rotational constants are slight modifications of the standard result[13]

$$\bar{\alpha}_k^\beta = -\left(\frac{2B_\beta^2}{\omega_k}\right)\left\{\sum_\gamma\left[\frac{3(a_k^{\beta\gamma})^2}{4I_{\gamma\gamma}}\right]+\sum_{l\neq k}^{F-1}(\xi_{kl}^\beta)^2\left(\frac{3\omega_k^2+\omega_l^2}{\omega_k^2-\omega_l^2}\right)+(\xi_{kF}^\beta)^2\left(\frac{3\omega_k^2-\bar{\omega}_F^2}{\omega_k^2+\bar{\omega}_F^2}\right)-\pi\left(\frac{c}{\hbar}\right)^{1/2}\left(\frac{f_{kkF}a_F^{\beta\beta}}{\bar{\omega}_F^2}-\sum_l^{F-1}\frac{f_{kkl}a_l^{\beta\beta}}{\omega_l^2}\right)\right\}. \tag{2.30}$$

As noted earlier, the rotational Hamiltonian in Eq. (2.25) can be diagonalized numerically for asymmetric tops. For approximately symmetric tops, it reduces to

$$E=V_0+\bar{E}_0+B_\perp J(J+1)+(B_\parallel-B_\perp)K^2+\sum_k^F[\omega_k-\alpha_k^\perp J(J+1)-(\alpha_k^\parallel-\alpha_k^\perp)K^2]\left(n_k+\frac{1}{2}\right)+\sum_{k\leqslant k'}^F x_{kk'}\left(n_k+\frac{1}{2}\right)\left(n_{k'}+\frac{1}{2}\right), \tag{2.31}$$

where $B_\parallel$ and $\alpha_k^\parallel$ correspond to the values of the unique axis and $B_\perp$ and $\alpha_k^\perp$ correspond to the average of the values of the perpendicular axes. This can be rewritten as a quadratic equation in θ with real coefficients and inverted to obtain

$$\theta(\mathbf{n},J,K;E)=\frac{2\pi\delta E/\tilde{\omega}_F}{1+\sqrt{1+4x_{FF}\delta E/\tilde{\omega}_F^2}}, \tag{2.32a}$$

where

$$\delta E\equiv V_0-E+\bar{E}_0+B_\perp J(J+1)+(B_\parallel-B_\perp)K^2+\sum_{k=1}^{F-1}[\omega_k-\alpha_k^\perp J(J+1)-(\alpha_k^\parallel-\alpha_k^\perp)K^2]\left(n_k+\frac{1}{2}\right)+\sum_{k\leqslant k'}^{F-1}x_{kk'}\left(n_k+\frac{1}{2}\right)\left(n_{k'}+\frac{1}{2}\right) \tag{2.32b}$$

$$\tilde{\omega}_F\equiv\bar{\omega}_F-\alpha_F^\perp J(J+1)-(\alpha_F^\parallel-\alpha_F^\perp)K^2-\sum_{k=1}^{F-1}\bar{x}_{kF}\left(n_k+\frac{1}{2}\right). \tag{2.32c}$$

Equation (2.32) combined with Eq. (2.21) provides the transition state labeled values of the transmission probability. This theory will break down when

$$\frac{4x_{FF}\delta E}{\tilde{\omega}_F^2}<-1, \tag{2.33}$$

which can result from either a resonance between the rovibrational modes or from too low an order in the perturbation treatment. In the former case, the offending resonant term can be treated at lower order and explicitly diagonalized.[14] In the latter case, a higher order perturbation treatment is required. While the energy expression can easily be obtained using symbolic manipulation with a computer,[16] the lack of higher order *ab initio* rovibrational coefficients in the potential presently prohibits this.

In summary, therefore, the normalized eigenvalues of Γ are given by

$$\gamma_\nu/\mathrm{Tr}(\Gamma)=P_\nu/N, \tag{2.34}$$

where $N(\equiv\Sigma_\nu P_\nu)$ is the cumulative reaction probability (CRP) and ν is a collective index of all the quantum numbers of the activated complex. With this association, Eq. (2.13) becomes

$$p(x)=(2\pi)^{-1}\int_{-\infty}^{\infty}dt\,e^{ixt}D(t)^{-1/2}, \tag{2.35a}$$

where

$$D(t)=\prod_\nu(1+2itP_\nu/N). \tag{2.35b}$$

Thus given an *ab initio* calculation of various "spectroscopic" parameters at the saddle point of the potential energy surface, one can readily calculate the transmission probabilities and subsequently use Eq. (2.35) in order to predict the reduced decay rate probability distribution. (The "spectroscopic" parameters include the frequencies and anharmonicities obtained from the quadratic, cubic, and a limited set of the quartic force constants; the rotational constants; and the α's in the Coriolis interaction.)

C. Symmetry considerations

The "good" quantum numbers associated with the transition states discussed above in Sec. II B are in general not globally conserved quantum numbers. If they were, the molecular Hamiltonian would be integrable, and thus certainly not chaotic, strongly mixed, etc. Most of the "good" quantum numbers of the transition state—e.g., the vibrational quantum numbers $\{n_k;k=1,...,F-1\}$—are good only in the transition state region and thus only relevant for approximating the eigenvalues of Γ. The total angular momentum J (in field-free space), however, is a *globally* conserved quantum number; consequently, states of different J are noninteracting. In applying any statistical theory, one should thus take cognizance of all globally conserved quantum numbers—e.g., total angular momentum (in field-free space), global discrete symmetries (the molecular symmetry group), etc.—and invoke the statistical assumption of strong mixing only *within* each manifold of states labeled by the globally conserved quantum numbers. How the globally conserved symmetries are included into RM/TST is the subject of the present analysis. The role of symmetry in statistical theories has been treated in other contexts by several authors.[17,18]

Therefore suppose that μ are the globally conserved quantum numbers and that ν are the quantum numbers conserved only locally in the transition state region. The eigenvalues $\gamma(\mu\nu)$ of the Γ matrix are labeled by the complete set of quantum numbers arising from the direct product of μ and ν. One then applies the RM/TST theory separately for each set of the conserved quantum numbers μ. The distribution of unimolecular decay rates for the μ manifold of strongly mixed states is thus given by [noting Eqs. (2.13a) and (2.35)]

$$P_\mu(\Gamma)\equiv\bar{\Gamma}_\mu^{-1}p_\mu(\Gamma/\bar{\Gamma}_\mu)$$
$$=(2\pi\bar{\Gamma}_\mu)^{-1}\int_{-\infty}^{\infty}dt\,e^{it\Gamma/\bar{\Gamma}_\mu}D_\mu(t)^{-1/2}, \quad (2.36a)$$

$$D_\mu(t)=\prod_\nu[1+2itP(\mu\nu)/N_\mu], \quad (2.36b)$$

where $\bar{\Gamma}_\mu$ is the average decay rate for the states in the μ manifold and $N_\mu[\equiv\Sigma_\nu P(\mu\nu)]$ is the cumulative reaction probability for the μ manifold. The combined or total distribution is the sum over all the μ distributions weighted by the density of states, i.e.,

$$P_{\rm tot}(\Gamma)=\sum_\mu f_\mu P_\mu(\Gamma) \quad (2.37)$$

with

$$f_\mu\equiv\frac{\rho_\mu}{\rho}, \quad (2.38)$$

where ρ_μ is the density of states of the μ manifold and ρ is the total density of states. This is rewritten in terms of the reduced distributions [Eq. (2.13)] as

$$p_{\rm tot}(x)=\sum_\mu f_\mu\frac{\bar{\Gamma}}{\bar{\Gamma}_\mu}p_\mu\left(x\frac{\bar{\Gamma}}{\bar{\Gamma}_\mu}\right). \quad (2.39)$$

Note that this distribution yields the usual transition state (or RRKM) expression for the average rate

$$\bar{\Gamma}=\sum_\mu f_\mu\bar{\Gamma}_\mu \quad (2.40a)$$

with

$$\bar{\Gamma}_\mu=N_\mu/(2\pi\rho_\mu). \quad (2.40b)$$

The total distribution can also be written, in terms of the cumulative reaction probabilities of the different μ manifolds, as

$$p_{\rm tot}(x)=\sum_\mu f_\mu\eta_\mu p_\mu(\eta_\mu x) \quad \text{and} \quad \eta_\mu\equiv\frac{f_\mu N}{N_\mu}. \quad (2.41)$$

Furthermore, the moments of the distribution can be written analytically in terms of the moments for each manifold as

$$\langle x^n\rangle=\sum_\mu f_\mu(\eta_\mu)^{-n}\langle x^n\rangle_\mu, \quad (2.42)$$

where $\langle\cdots\rangle_\mu$ denotes an average with respect to $p_\mu(x)$.

A simple example of these expressions results when the only underlying symmetry divides the states into two uncoupled manifolds, each with an equal density of states. This does not necessarily imply that the corresponding CRPs are equal as the states in a given manifold access only the transition states labeled by the corresponding global symmetry of the manifold. (This case is actually physically relevant as it can arise if the molecular symmetry group is C_s.) Equation (2.41) becomes

$$p_{\rm tot}(x)=\frac{1}{4}\left[\frac{N}{N_1}p_1\left(x\frac{N}{N_1}\right)+\frac{N}{N_2}p_2\left(x\frac{N}{N_2}\right)\right] \quad (2.43)$$

and Eq. (2.42) becomes

$$\langle x^n\rangle=2^{n-1}\left[\left(\frac{N_1}{N}\right)^n\langle x^n\rangle_1+\left(\frac{N_2}{N}\right)^n\langle x^n\rangle_2\right]. \quad (2.44)$$

This expression with $n=2$ can be used to obtain the effective number of channels

$$\frac{2}{\nu_{\rm eff}}=\frac{4(N_1^2/\nu_{{\rm eff},1}+N_2^2/\nu_{{\rm eff},2})}{(N_1+N_2)^2}+\frac{(N_1-N_2)^2}{(N_1+N_2)^2}, \quad (2.45)$$

where $\nu_{{\rm eff},i}$ is the effective number of channels for the i manifold.

Thus in order to predict a decay rate probability distribution for a given system, one first searches for any conserved symmetries or quantum numbers. Equation (2.36) is used to obtain the distribution for each of the symmetry blocks. These are combined using Eq. (2.41) to obtain the final result. Note that if only the moments are desired, then one first uses the $\gamma(\mu\nu)$'s to obtain $\langle x^n\rangle_\mu$ analytically [e.g., Eq. (2.11) for the second moment] and then use of Eq. (2.42) provides the symmetry adapted RM/TST moments directly. This can also provide a useful check on the numerical evaluation of the probability distribution.

III. APPLICATION TO FORMALDEHYDE

In order to apply the random matrix/transition state theory developed in the previous section to D_2CO, the quartic potential and rovibrational constants must be known at the transition state. However, as Schneider and Thiel[19] observed for bound state systems, the only quartic derivatives needed to obtain the x_{ij}'s are those of the form f_{kkll}. Handy and co-workers[20] have shown that all of the cubic derivatives and this limited set of quartic derivatives can be calculated efficiently by central differences of analytic second derivatives obtained at second order Møller–Plesset theory (MP2).[21] This method was directly applicable to the determination of the perturbed Hamiltonian near the transition state and results for the $(J=0)$-D_2CO transmission probabilities indicate that there is a small, but measurable effect due to the anharmonicity.[12]

The coefficients needed for the rovibrational Hamiltonian are listed in Table I.[22] Since the transition state geometry of D_2CO is a near prolate symmetric top—c.f., the asymmetry parameter is

$$\kappa\equiv\frac{2B-A-C}{A-C}=-0.95 \quad (3.1)$$

—its rotational energy levels were approximated as a symmetric top. (The rotational constants used for the $\perp$ direction are taken to be the average of the x and y directions.)

A. The reduced probability distributions

Before comparing to experiment, it is useful to study the degree to which the RM/TST distributions depend on energy and dynamical symmetries. As pointed out in Sec.

TABLE I. The coefficients of the rotational Hamiltonian expanded about the saddle point of the D_2CO potential energy surface (Refs. 12 and 22). The rotational constants are $B_x=0.76$, $B_y=0.89$, and $B_z=5.59$. All values are in units of cm^{-1}.

		$x_{k,k'}$								
k	ω_k	$k'=1$	$k'=2$	$k'=3$	$k'=4$	$k'=5$	$k'=6$	α_k^x	α_k^y	α_k^z
$1(a')$	2478	−15.1						−0.001	−0.002	−0.004
$2(a')$	1730	−19.6	−7.6					−0.002	−0.002	−0.011
$3(a')$	1125	1.1	−16.0	−13.8				−0.003	−0.0002	−0.162
$4(a'')$	698	−14.9	2.0	−4.2	−3.1			0.000	−0.0003	−0.624
$5(a')$	660	0.9	−16.8	−1.0	2.0	−2.0		0.003	−0.002	0.529
$6(a')$	1579i	57.1i	3.3i	−14.6i	28.2i	−3.0i	−6.7	0.0003i	0.0006i	0.075i

II C, a given system can consist of noninteracting manifolds of states which will not be strongly mixed due to symmetry. For formaldehyde in a Stark field, the only rigorously conserved quantum number is M, the projection of total angular momentum onto the constant electric field (space fixed) direction. In field-free space, to the extent that the mixing of states caused by the Stark field is negligible, the total angular momentum J and the molecular symmetry[23] C_s are also globally conserved. Since D_2CO is a near symmetric top, there is also the question of whether K—the projection of J onto the body-fixed axis—is better described as strongly mixed or (approximately) conserved globally. Since $+|K|$ and $-|K|$ states are used to obtain the C_s symmetry adapted states, one can at most require the conservation of $|K|$. [The conditions for labeling a given transition state as even (A') or odd (A'') are given in Miller.[24] Note that ν_4 the out-of-plane mode, is the only vibrational mode which is nontrivial with respect to C_s symmetry.]

Thus four cases of dynamical symmetry which are pertinent to the D_2CO dissociation are:

(a) *J and M* are the conserved quantities;
(b) *J, M, and C_s* are the conserved quantities;
(c) *J, M, $|K|$,* and *C_s* are the conserved quantities;
(d) *M and C_s* are the conserved quantities with J partially broken and $|K|$ less so.

Although case (d) is potentially very relevant to the dynamics, we cannot use the present form of RM/TST to obtain the corresponding distributions since it would require the use of "partially" mixed states. For the remaining cases, we can construct *J-resolved* distributions, i.e.,

$$p_{J,M}(x)=\sum_{\mu} f_{J,M,\mu}\frac{\bar{\Gamma}}{\bar{\Gamma}_{J,M,\mu}}p_{J,M,\mu}\left(x\frac{\bar{\Gamma}}{\bar{\Gamma}_{J,M,\mu}}\right), \qquad (3.2)$$

where $p_{J,M,\mu}$ are the RM/TST reduced probability distributions labeled by J, M, and μ, and the sum is over all values of μ which are *accessed* in the experiment. (In the symmetric top limit, the transmission probabilities are independent of M and consequently so is the J-resolved distribution; $p_{J,M}=p_J$.)

In case (a), the sum in Eq. (3.2) collapses into a single term—Eq. (2.36) labeled by J and M. In the remaining cases, it is also necessary to make an assumption on the μ states accessed by the experiment and consequently included in the sum in Eq. (3.2). In case (b), we make the most democratic choice by including all such states. Since states in A' or A'' will have essentially the same density of states, the J-resolved distribution in case (b) is obtained using Eq. (3.2) with $f_i=\frac{1}{2}$, in analogy to Eq. (2.43). In case (c), if $|K|$ is conserved in the preparation of the metastable states, then only those states with $|K|=J$ will be observed in the experiments. With this restriction, the sum in Eq. (3.2) only includes the two C_s states corresponding to $|K|=J$ and it reduces to Eq. (2.43) as in case (b).

In Figs. 2–4, the RM/TST J-resolved reduced probability distributions are presented at selected sample energies relative to the bare barrier and for different values of J. (The energies are chosen to sample energy regimes well below, just above, and well above the zero point energy adjusted barrier.) The figures indicate that there is a pronounced variation in the shape of the predicted distributions as a function of E, J, and symmetry. In particular, the distributions tend to be narrower and more strongly

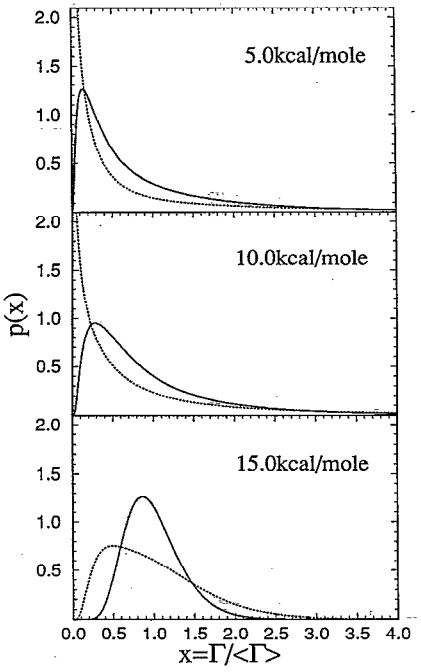

FIG. 2. RM/TST probability distributions with $J=0$ at various energies. The *solid* curves are obtained assuming no additional conserved quantities [case (a)]. The *short-dashed* curves are obtained assuming that C_s symmetry is also obeyed [case (b)].

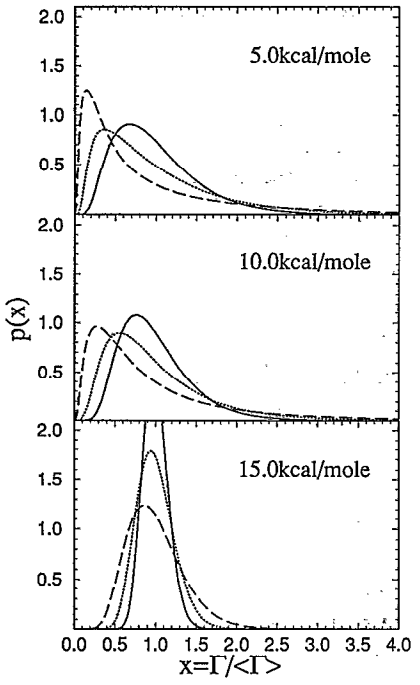

FIG. 3. RM/TST probability distributions with $J=2$ at various energies. The *solid* and *short-dashed* curves correspond to the same cases as in Fig. 2. The *long-dashed* curves are obtained assuming that C_s symmetry and $|K|$ are also obeyed [case (c)].

peaked with either increasing energy or decreasing dynamical symmetry.

ν_{eff} is often used to characterize these probability distributions by a single parameter. However, one should be careful not to rely too heavily on this measure. One reason

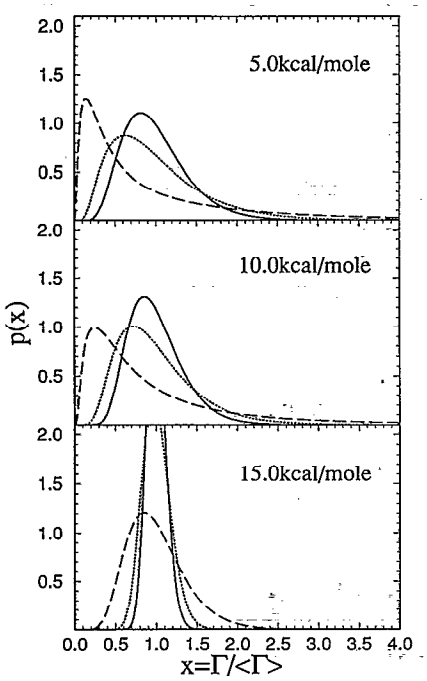

FIG. 4. RM/TST probability distributions with $J=4$ at various energies. All curves correspond to the same cases as in Figs. 2 and 3.

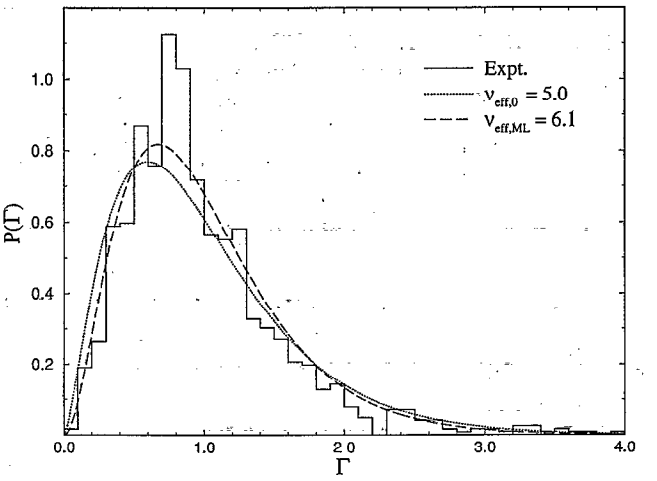

FIG. 5. χ^2 distributions with various values of ν_{eff} vs the experimental histogram (Ref. 3).

for this is that very different distributions can have the same value of ν_{eff} as illustrated in Ref. 2. A second reason is that if Eq. (2.12) is used to obtain ν_{eff} for a finite number of observables—we refer to this value as ν_{eff}^0—then the largest rates will bias the value of ν_{eff}^0 unequally. Moreover, large rates correspond to broader peaks which are poorly resolved experimentally. In order to account for this, one can use the maximum-likelihood method[25,26] to define ν_{eff}. The standard result for p observables is that $\nu_{\text{eff}}^{\text{ML}}$ satisfies

$$F(\nu_{\text{eff}}^{\text{ML}}/2)=\frac{1}{p}\sum_{i=1}^{p}\ln(\Gamma_i/\bar{\Gamma}), \tag{3.3a}$$

where

$$F(z)\equiv\frac{\partial G}{\partial z}-\ln z \tag{3.3b}$$

and G is the logarithm of the gamma function.

In Fig. 5, the experimental histogram for all the D_2CO decay rates is compared to χ^2 distributions with ν_{eff} determined by ν_{eff}^0 and $\nu_{\text{eff}}^{\text{ML}}$. It should be clear that while the difference in these calculated values of ν_{eff} is large, the difference between the two χ^2 distributions is small. Although both distributions are in reasonable agreement with the experimental result (the histogram), one can discern qualitative differences, e.g., the experimental distribution is narrower and dies off faster at the high end.

Equation (3.3) is exact if the distribution is a χ^2 distribution with $\nu_{\text{eff}}^{\text{ML}}$ degrees of freedom. However, in general, the RM/TST distribution will differ from a χ^2 distribution and consequently the corresponding values of $\nu_{\text{eff}}^{\text{ML}}$ and ν_{eff}^0 will also differ. Since the difference between these measures is small compared to the error in the experimental values, we will simply present the values of the RM/TST ν_{eff}^0's for comparison in what follows.[27]

TABLE II. The cumulative reaction probability for the J-resolved and combined probability distributions compared to experiment (Ref. 3).

	RM/TST[a]	RM/TST[b]	Exp.[c]	Exp.[d]	Exp.[e]
$N_{J=1}$	0.98	1.97	3.47	1.36	1.36
$N_{J=2}$	1.59	1.90	4.09	1.60	1.50
$N_{J=3}$	2.13	1.78	6.31	2.46	1.72
$N_{J=4}$	2.58	1.63	9.76	3.81	2.70
$\Sigma_J N_J$	7.28	7.28	23.63	9.22	7.28
$2\pi\rho\bar{\Gamma}$	7.28	7.28	23.11	9.02	7.13

[a]For case (b).
[b]For case (c).
[c]Using $\rho(J)=(2J+1)\rho_{\exp}(0)$.
[d]Using $\rho(J)=(2J+1)\rho_{\exp}(1)/3$.
[e]Using $\rho(J)=\rho_{\exp}(J)$ in the case that K is predominantly conserved.

B. D_2CO barrier height

In the previous section, the RM/TST distributions were shown to vary strongly with the energy relative to the bare barrier

$$E=h\nu_{\exp}+E^0_{\mathrm{ZPE}}-V_0, \tag{3.4}$$

where $\nu_{\exp}$ is the frequency of the excitation in the experiment, E^0_{ZPE} is the zero point energy (ZPE) of the bound state, and V_0 is the bare barrier height. Since the theoretical calculations are performed about the barrier, the values of E^0_{ZPE} and V_0 are required in order to match the experiment. E^0_{ZPE} is readily computed from the ground state force field of formaldehyde; the force field has been computed by Handy *et al.*[20] using analytic second derivatives within MP2 and compares well with the experimental results of Duncan and Mallinson[28] and Reisner *et al.*[29] (For D_2CO, $E^0_{\mathrm{ZPE}}=13.0$ kcal/mol.) However, *ab initio* calculations are just beginning to reach agreement on V_0 (Ref. 30) and it is useful to obtain an estimate of the barrier height by a fit of the J-resolved experimental results with the semiclassical anharmonic transition state model described in Sec. II B.

The barrier height can be determined by varying the energy of the RM/TST cumulative reaction probability (CRP) calculation until agreement is reached with the experimentally inferred CRP. The latter quantity can be obtained, in principle, by either of two equivalent methods. The most straightforward is to write

$$N=2\pi\rho\bar{\Gamma} \quad \text{with} \quad \rho=\sum_J \rho_J. \tag{3.5a}$$

Alternatively, the CRP is the sum

$$N=\sum_J N_J=2\pi\sum_J \rho_J\bar{\Gamma}_J. \tag{3.5b}$$

The two methods are clearly equivalent if $\bar{\Gamma}$ is the weighted average of $\bar{\Gamma}_J$ as in Eq. (2.40). The extent to which these expressions are not equal is therefore a consistency check on the experimentally[1] obtained rates and density of states $\rho_{\exp}(J)$. In general, one also needs to include the appropriate symmetry numbers in the rate expressions.[23] This is hidden in Eq. (3.5) and subsequent expressions by including the symmetry numbers in the density of states.

A difficulty in carrying out this procedure arises from the nature of the Stark level-crossing spectroscopy experiment. S_0 resonances are necessarily observed at varying electric field strengths, giving rise to a density of state anomaly which is not directly accounted for in the calculation. The density of S_0 vibrational states is observed to increase by a factor of 4 over a typical electric field strength scan of 20 kV/cm.[1] This increase in density of states is attributed to partial breakdown of the J quantum number. The varying density of states introduces an uncertainty in the determination of the experimental CRP and hence in the calculated decay rate distributions. To limit this effect, the density of states used in the CRP calculation is obtained by extrapolating the observed density of states to zero electric field.[1] Although all of the data are used to obtain the average rate, a restriction to those rates obtained at low electric field yields at most a 0.2 kcal/mol lowering in the barrier height, thus suggesting that the electric field has a small effect on the average rate.

Since cases (b) and (c) are the most likely candidates describing the dynamics of the reaction at zero electric field, only these cases are considered in calculating the barrier height. In case (c), the restriction to include only the $|K|=J$ states lowers the CRP relative to that of case (b), and consequently a lower barrier is needed to fit to the experimental value. Thus a fit to the experimentally inferred CRP also provides some information about the metastable states which are being accessed by the experiment.

If all the K states are accessed in the experiment, as in case (b), then the density of states is given by a state count, i.e.,

$$\rho(J)=(2J+1)\rho(0), \tag{3.6}$$

where $\rho(J)$ is the density of states as a function of J. The density of states is thus determined by a single multiplicative constant; the first two experimental columns in Table II present the results of this calculation with either $\rho_{\exp}(0)$ or $\rho_{\exp}(1)$ fixing this multiplicative constant. [Note that $\rho_{\exp}(0)$ is a further extrapolation of the observed $\rho_{\exp}(J)$ assuming linear dependence with a slope of (0.45 ± 0.16) instead of the statistical value of 2.[1]] If only the $|K|=J$ states are accessed in the experiment, as in case (c), then the density of states will be independent of J. However, the density of states observed experimentally by Polik *et al.*[1] did not quite follow either of these statistical regimes. In fact, they found that "although the density of states increases slightly with J, K appears to be predominantly conserved."[1] The last experimental column in Table II presents the CRPs obtained using $\rho_{\exp}(J)$. The relative ratios in the calculation of the total CRP using Eqs. (3.5a) and (3.5b) between each of the experimental columns of Table II are similar, and thus this consistency check does not resolve the issue of which is the correct choice of the density of states.

The RM/TST CRPs presented in Table II are obtained at a value of the barrier height such that the total CRP agrees with the experimentally inferred CRP using $\rho_{\exp}(J)$. In case (b), the CRP is fit to the third experimental col-

TABLE III. *Ab initio* and empirical bare barrier heights in units of kcal/mol for the $D_2CO \rightarrow D_2 + CO$ reaction.

Method	Barrier height	Reference
MCSCF+CI	86.0±2.5	31
MP4SDTQ	85.9	32
CCSDT-1	86.8	30
RRKM ($J=0$)	84.6±0.8	1
RM/TST (b)	85.4±1.0	...
RM/TST (c)	84.1±1.0	...

umn with $V_0=85.4\pm1.0$ kcal/mol; a decrease in the barrier height by 0.2 kcal/mol would increase the total CRP to match that of the second experimental column, whereas a 1.3 kcal/mol decrease is required to match the first. In case (c), the CRP is fit to the third experimental column with $V_0=84.1\pm1.0$ kcal/mol; a decrease in the barrier height by 0.3 kcal/mol would increase the total CRP to match that of the second experimental column, whereas a 2.3 kcal/mol decrease is required to match the first. In both sets of cases, the error arises from the same sources as in Ref. 1 with an additional 0.2 kcal/mol arising from the energy spread of the observed rates. Assuming that the dependence of the density of states on J is correct in the experiments, then the barrier heights are taken to be those which matched the third experimental column. In any event, we note that a change in the RM/TST distributions caused by up to a 0.5 kcal/mol decrease of the barrier height does not significantly alter the *qualitative* features of the RM/TST distributions.

In Table III, the RM/TST results for the bare barrier are summarized and compared to previous *ab initio* results and to the earlier result of Polik *et al.*[1] obtained using a harmonic RRKM fit of all of the rates extrapolated to $J=0$. The RM/TST barrier heights are within the error bars of the $J=0$ extrapolation. Although the result under case (b) is closer to the *ab initio* results than that for case (c), the agreement is insufficient to conclude that all the K states are accessed in the experiment.

C. Comparison to experiment

A comparison between the RM/TST and experimental reduced probability distributions should reveal which local quantum numbers are approximately conserved throughout the reaction and which are strongly mixed. In case (b), e.g., the energy of the experiment relative to the bare barrier is 8.7 kcal/mol. Since this is near the zero point energy of the transition state ($\sim$9.5 kcal/mol), many of the contributing transition states are in the tunneling regime and an adequate description of their transmission probabilities must account for tunneling and anharmonicity. This, therefore, justifies the need for the semiclassical transition state model described in Sec. II B.

The J-resolved RM/TST distributions are compared to the experimental histograms for individual J states[1,3] in Fig. 6. [Note that in case (a), the calculations are performed using the barrier height obtained in case (b).] The poor agreement between the histograms and distributions

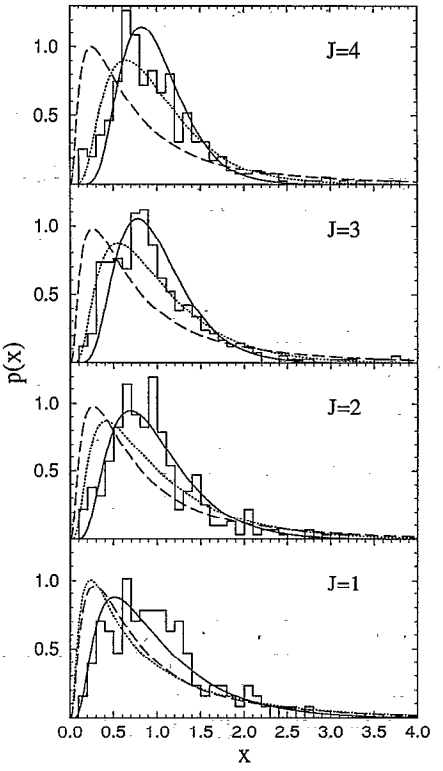

FIG. 6. RM/TST probability distributions at the energy of the experiment for various values of J compared to the J-resolved experimental histograms (Refs. 1 and 3). The *solid*, *short-dashed*, and *long-dashed* curves are the same as in Figs. 2 and 3.

obtained for case (c) indicates that $|K|$ is *not* conserved. The experimental distribution seems to lie in between the theoretical distributions for cases (a) and (b), and this suggests that the system has some mixing between the C_s states, but not complete mixing. For completeness, the values of ν_{eff} for cases (a), (b), and (c) are compared to ν_{eff}^0 and $\nu_{\text{eff}}^{\text{ML}}$ in Table IV. As is the case for the total distribution, there is disagreement between the experimentally determined values ν_{eff}^0 and $\nu_{\text{eff}}^{\text{ML}}$ providing further support for their limited utility. Nonetheless, the experimentally obtained values roughly fall in between the RM/TST results for cases (a) and (b). It should also be noted that to a good approximation, the primary effect of C_s symmetry is to halve the available transition states (i.e., $\nu_{\text{eff},a} \approx 2\nu_{\text{eff},b}$) and this is seen in the RM/TST results in Table IV. Thus, the J-resolved results indicates that the K states are strongly mixed and that C_s symmetry is to some extent broken, but not completely mixed in the random matrix sense.

In order to combine the J-resolved RM/TST distributions using Eq. (2.41), the relative density of states of each J manifold must be determined. The combined RM/TST distributions using either the statistical density of states, where $\rho(J)=(2J+1)\rho(0)$, or the experimental densities of states $\rho_{\text{exp}}(J)$ are compared to the experimental histogram in Fig. 7. As was the case for the J-resolved distributions, the total RM/TST distributions for cases (a) and (b) bracket the observed histogram, while the distribution

TABLE IV. The values of ν_{eff} for the J-resolved and combined probability distributions. ν^0_{eff} is computed from the experiments using Eq. (2.12). $\nu^{\text{ML}}_{\text{eff}}$ is obtained using the maximum-likelihood method (Ref. 26). $\nu^0_{\text{eff},a}$, $\nu^0_{\text{eff},b}$, and $\nu^0_{\text{eff},c}$ are the RM/TST results under cases (a), (b), and (c), respectively.

	All rates		Low E field		High E field		RM/TST		
J	ν^0_{eff}	$\nu^{\text{ML}}_{\text{eff}}$	ν^0_{eff}	$\nu^{\text{ML}}_{\text{eff}}$	ν^0_{eff}	$\nu^{\text{ML}}_{\text{eff}}$	$\nu^0_{\text{eff},a}$	$\nu^0_{\text{eff},b}$	$\nu^0_{\text{eff},c}$
1	7.0	6.8±1.0	5.2	4.5±1.6	7.4	7.8±1.4	4.61	2.12	2.08
2	4.0	6.0±1.5	2.0	3.6±1.0	8.0	8.4±1.7	7.66	3.63	2.04
3	4.7	6.3±0.9	3.3	4.2±1.5	9.2	9.0±1.4	10.7	5.11	1.97
4	6.2	6.9±1.1	5.3	6.0±1.4	7.7	7.6±1.2	13.6	6.55	1.89
All	5.0	6.1±0.7	3.4	4.3±0.9	7.4	7.7±0.8	8.70[a]/8.70[b]	4.14[a]/4.25[b]	1.35[a]/1.63[b]

[a]Obtained using $(2J+1)$ weights.
[b]Obtained using the experimentally observed density of states $\rho_{\text{exp}}(J)$ in the case that K is predominantly conserved.

for case (c) is shifted somewhat to the left of the experimental histogram. This once again leads to the possible conclusion that states of different C_s symmetry are partially mixed by the Stark field.

While the above calculations suggest total breakdown of the $|K|$ quantum number as a candidate for the origin of the additional degrees of freedom observed in the experimental decay rate distributions, it is acknowledged that several other potential sources for degrees of freedom also exist. First, vibrational anharmonicity arising from still higher order terms in the transition state region of the potential energy surface could result in a higher ν_{eff}.[2] Second, J breakdown induced by the Stark field will increase the number of available decay channels and could provide similar agreement between experimental and calculated distributions. Third, only the limiting cases of no breakdown or complete breakdown of the $|K|$ quantum number have been considered in this treatment. An intermediate case—e.g., case (d)—of partial K breakdown, in combination with other decay channels, could account for the experimental distributions. Note that this would increase the barrier height—although by less than 1.0 kcal/mol—because the sum in the CRP would now include additional states of the activated complex. While the intent of this paper has been to examine the decay rate distributions observed in S_0 D_2CO, other experimental data suggest that $|K|$ may not be strongly mixed. The lack of a $2J+1$ dependency of the experimental density of states and the lack of a $1/(2J+1)$ dependency of the average squared S_1–S_0 coupling matrix element each suggest that $|K|$ is only partially mixed.[1]

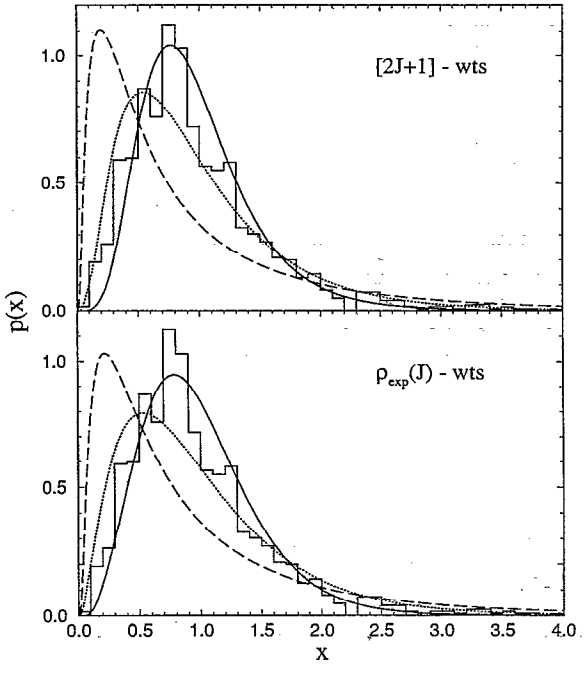

FIG. 7. RM/TST probability distributions at the energy of the experiment with $\rho(J)=(2J+1)\rho_{\text{exp}}(0)$ and with $\rho(J)=\rho_{\text{exp}}(J)$ compared to the experimental histogram for all rates. The *solid, short-dashed,* and *long-dashed* curves are obtained assuming cases (a), (b), and (c), respectively.

Thus far, the effect of the electric field on the rates has been ignored since the energetic effect is minimal. However, the isotropy of space is broken in the presence of an electric field and this minimally breaks the C_s symmetry in the molecule-fixed frame of the transition state at sufficiently high field strengths. The loss of C_s symmetry can have a strong effect on the statistical distributions as evidenced by the difference in the RM/TST distributions in Fig. 7. In fact, the results for cases (a) and (b) might suggest that at low electric field strengths, C_s symmetry would be conserved, whereas at high electric field strengths, it would be broken. This is further suggested, e.g., in Fig. 10 of Ref. 3, in which ν_{eff} is plotted vs electric field; although a linear fit is shown in that presentation, its behavior is more like that of a sigmoid with ν_{eff} going from $\sim$4 in the low field region to $\sim$8 in the high field region. The ratio of two in ν_{eff} between these two regions indicates that the electric field is breaking a symmetry which has only two labels, such as C_s symmetry.

In Fig. 8(a), the experimental histogram is obtained using all of the 212 observed rates with electric field strength less than 6.5 kV/cm and is compared to the RM/TST distributions with C_s symmetry. In Fig. 8(b), the experimental histogram is obtained using all of the 617 observed rates with electric field strength greater than 12.0 kV/cm and is compared to the RM/TST distributions without C_s symmetry. Although not shown, the histograms labeled by J for each of these electric field cases were also compared to the J-resolved distributions yielding analogous agreement. In addition, the values of ν_{eff} for these electric field cases are also compared to the RM/TST val-

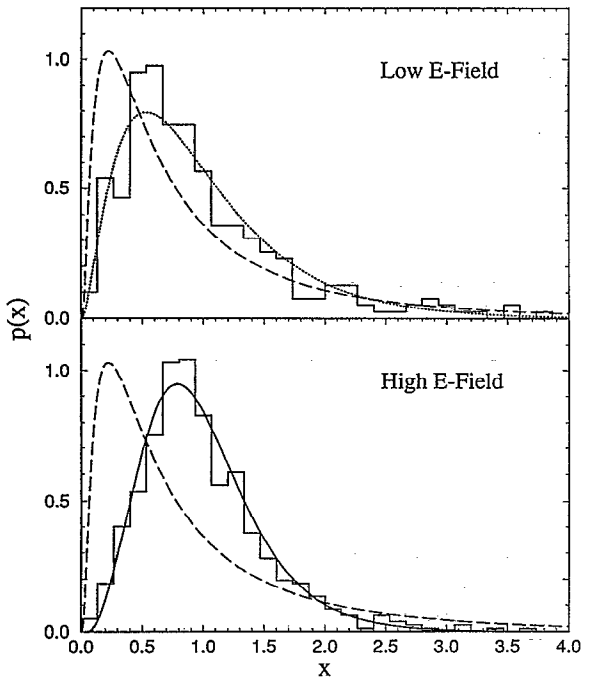

FIG. 8. RM/TST probability distributions at the energy of the experiment compared to the experimental histogram for rates at low electric field and at high electric field. The RM/TST distributions are obtained with $\rho(J)=\rho_{\rm exp}(J)$, and the *solid, short-dashed,* and *long-dashed* curves are obtained as in Fig. 7.

ues in Table IV. The agreement is remarkable and suggests that C_s symmetry is approximately conserved at low electric field, while at sufficiently high electric field, the symmetry is completely broken. Nonetheless, while this markedly different behavior in the experimental distributions is mimicked by the breaking of C_S symmetry, the possibility that the breakdown of J by the Stark field could account for this behavior has not been ruled out.

IV. CONCLUDING REMARKS

It may be helpful to recap briefly the basic assumptions behind the derivation of the RM/TST model [Eq. (2.13) in Sec. II A]. (a) The imaginary part of the effective Hamiltonian matrix (2.1) is treated by first order perturbation theory; this is essentially the assumption that the resonances are nonoverlapping ($\Gamma_k < |E_k - E_{k'}|$ on the average). (b) The real part of the effective Hamiltonian matrix (2.1) is assumed to be a "random" matrix,[4] i.e., the quantum states are assumed to be *strongly mixed* ("chaotic"). (The only result of random matrix theory which is actually used is that the projections of the eigenstates onto an arbitrary basis are Gaussian random numbers.) Assumption (a) is not very severe since under assumption (b) the state-selected decay rates would be experimentally accessible only if the resonances were nonoverlapping or weakly overlapping. However, assumption (b) can hold only if the effective number of mixed states f is large enough that the association specified by Eq. (2.7) will hold; this can only happen in a region with a high density of states. Thus this analysis is applicable in an intermediate energy regime in which there is a balance between a high density of states and resolvable widths.

The primary new development of the RM/TST model is the generalization to include globally conserved quantities (e.g., total angular momentum and discrete molecular symmetries). Use of the semiclassical transmission probabilities described in Sec. II B also converts this model into a predictive theory. The probability distribution of unimolecular decay rates that results from this RM/TST theory can depend sensitively on which degrees of freedom one assumes are strongly mixed and which are approximately conserved. In practice, therefore, one carries out the statistical calculation for various such assumptions and compares to experimental results to deduce information about the unimolecular dynamics.

Application of the RM/TST theory to the distribution of state-specific unimolecular decay rates of D_2CO for individual values of total angular momentum J shows quite good agreement with the experimental results of Polik *et al.*[1] In particular, if one assumes that all of the K states are accessed in the experiment and that $|K|$ is strongly mixed, one obtains very good agreement between RM/TST and the experiment; the differences between the low and high field distributions may be attributable to the breaking of C_s symmetry by the Stark field. However, this agreement may be deceptive in that previous analysis[1,3] of the experimental data suggest that $|K|$ is not strongly mixed. In this case, the RM/TST results suggest that if one is to treat $|K|$ as conserved, then one must allow J to break down. Thus while this work does not unambiguously resolve the issue as to which rovibrational states are strongly mixed, there seems little doubt that some states are strongly mixed and that the Stark field is inducing further mixing.

ACKNOWLEDGMENTS

This work is supported by the Director, Office of Energy Research, Office of Basic Energy Sciences, Chemical Sciences Division of the U.S. Department of Energy under contract No. DE-AC03-76SF00098. C.B.M. acknowledges support from the National Science Foundation (CHE 8816552). R.H. acknowledges port from the National Science Foundation and the AT&T Cooperative Research Fellowship Program for predoctoral fellowships. W.F.P. acknowledges support from Research Corporation (C-2441R) and the National Science Foundation (CHE-9157713). We thank Nicholas C. Handy and Andrew Willetts for numerous helpful discussions and for providing us with the rovibrational constants at the saddle point of the D_2CO potential energy surface.

APPENDIX A: THE MICROCANONICAL QUANTUM SURVIVAL PROBABILITY

The "microcanonical quantum survival probability" is defined as a sum over a continuum of states with exponential decay, e.g.,

$$P(t)=\int_0^\infty d\Gamma\, P(\Gamma)e^{-\Gamma t}. \tag{A1}$$

This would correspond to the survival probability of a broadband excitation or collision experiment in which a dense set of exponentially decaying excited states are prepared uniformly in a narrow energy interval. Miller[7] and Hase[8] have considered this quantity explicitly for the case of Porter–Thomas distributions for $P(\Gamma)$. With the more general result for $P(\Gamma)$ given by RM/TST [Eq. (2.35) above], it is relatively straightforward to obtain the following result for $P(t)$:

$$P(t)=\prod_j [1+2t\bar{\Gamma}\gamma_j/\mathrm{Tr}(\Gamma)]^{-1/2}. \tag{A2}$$

If all the γ_j's are the same, then Eq. (A2) reduces to that given previously[7] for a χ-square distribution.

Equation (A2) can also be written as

$$P(t)=\prod_n \left(1+\frac{N_n t}{\pi\rho}\right)^{-1/2}, \tag{A3}$$

which is readily computed using the semiclassical transmission probabilities described in Sec. II B. In the limit that $t\to 0$, this equation reduces to

$$P(t)\approx \prod_n \left(1-\frac{1}{2}\frac{N_n t}{\pi\rho}\right)\approx\left(1-\sum_n \frac{N_n t}{\pi\rho}\right)\approx(1-\bar{\Gamma}t)\approx e^{-\bar{\Gamma}t}, \tag{A4}$$

which demonstrates in the short time limit the exponential falloff of the survival probability as determined by the average rate.

APPENDIX B: RELATION BETWEEN *f* AND ϵ

The value of the proportionality constant ϵ in Eq. (2.14) can be related to the effective number of mixed states f in RM/TST theory. Recall that the microcanonical rate is simply related to the cumulative reaction probability N and the density of states ρ by

$$\bar{\Gamma}=\frac{N}{2\pi\rho}. \tag{B1}$$

Equation (2.10) then gives

$$f=\frac{\mathrm{Tr}(\Gamma)}{\bar{\Gamma}}=\frac{\Sigma_n\gamma_n}{N/2\pi\rho}=2\pi\rho\epsilon\left(\frac{\Sigma_n N_n}{N}\right)=2\pi\rho\epsilon. \tag{B2}$$

If the states are not mixed, then $f=1$ and $\epsilon=(2\pi\rho)^{-1}$ as expected. In this case, ϵ is the average energy spacing. If the states are mixed, then f characterizes the average number of mixed levels and ϵ is the average energy spacing which contains f states.

Calculation of $\mathrm{Tr}(\Gamma)$ could thus provide a direct check on the applicability of RM/TST theory with large f being favorable. While this calculation is not within reach at present the relation specified in Eq. (B2) demonstrates that the notion of a set of strongly mixed states in a given energy interval is consistent with the semiclassical model described in Sec. II B; the size of that interval being ϵ.

[1] W. F. Polik, D. R. Guyer, and C. B. Moore, J. Chem. Phys. **92**, 3453 (1990).
[2] W. H. Miller, R. Hernandez, C. B. Moore, and W. F. Polik, J. Chem. Phys. **93**, 5657 (1990).
[3] W. F. Polik, D. R. Guyer, W. H. Miller, and C. B. Moore, J. Chem. Phys. **92**, 3471 (1990).
[4] See, e.g., (a) C. E. Porter, *Statistical Theories of Spectra: Fluctuations* (Academic, New York, 1965); (b) T. A. Brody, J. Flores, J. B. French, P. A. Mello, A. Pandey, and S. S. Wong, Rev. Mod. Phys. **53**, 385 (1981).
[5] H. Feshbach, Annu. Rev. Nucl. Sci. **8**, 49 (1958); Ann. Phys. **5**, 357 (1958); **19**, 287 (1962).
[6] D. F. Heller, M. L. Elert, and W. M. Gelbart, J. Chem. Phys. **69**, 4061 (1978).
[7] W. H. Miller, J. Phys. Chem. **92**, 4261 (1988).
[8] D.-h. Lu and W. L. Hase, J. Chem. Phys. **90**, 1557 (1989).
[9] T. Carrington, L. M. Hubbard, H. F. Schaefer, and W. H. Miller, J. Chem. Phys. **80**, 4347 (1984).
[10] W. H. Miller, N. C. Handy, and J. E. Adams, J. Chem. Phys. **72**, 99 (1980).
[11] W. H. Miller, Faraday Discuss. Chem. Soc. **62**, 40 (1977).
[12] W. H. Miller, R. Hernandez, N. C. Handy, D. Jayatilaka, and A. Willetts, Chem. Phys. Lett. **172**, 62 (1990).
[13] D. Papousek and M. R. Aliev, *Molecular Vibrational–Rotational Spectra* (Elsevier, Amsterdam, 1982).
[14] M. J. Cohen, N. C. Handy, R. Hernandez, and W. H. Miller, Chem. Phys. Lett. **192**, 407 (1992).
[15] M. Wolfsberg, J. Chem. Phys. **50**, 1484 (1969).
[16] E. L. Sibert, J. Chem. Phys. **88**, 4378 (1988); **90**, 2672 (1989).
[17] See, e.g., (a) P. Pechukas in *Modern Theoretical Chemistry*, edited by W. H. Miller (Plenum, New York, 1976), Vol. 2, p. 285 *et seq*; (b) P. R. Bunker, in *Vibrational Spectra and Structure*, edited by J. R. Durig (Marcel Dekker, New York, 1975), Vol. 3, pp. 1–126; (c) M. Quack, Mol. Phys. **34**, 477 (1977).
[18] W. H. Miller, J. Am. Chem. Soc. **105**, 216 (1983).
[19] W. Schneider and W. Thiel, Chem. Phys. Lett. **157**, 367 (1989).
[20] W. H. Green, A. Willetts, D. Jayatilaka, and N. C. Handy, Chem. Phys. Lett. **169**, 127 (1990); W. H. Green, D. Jayatilaka, A. Willetts, R. D. Amos, and N. C. Handy, J. Chem. Phys. **93**, 4965 (1990).
[21] C. Møller and M. S. Plesset, J. Chem. Phys. **46**, 618 (1934).
[22] A. Willetts and N. C. Handy (private communication).
[23] C_s is the symmetry of the transition state and the related reaction path. There are actually two (symmetrically equivalent) such transition states and they combine to give a molecular symmetry for D_2CO as C_{2v}. Because these two transition states are far enough apart to be noninteracting, one can use the lower symmetry C_s as we do here (Ref. 18).
[24] W. H. Miller, J. Phys. Chem. **87**, 2731 (1983). Note that in this reference, the out-of-plane mode is labeled as ν_5.
[25] C. E. Porter and R. G. Thomas, Phys. Rev. **104**, 483 (1956).
[26] R. D. Levine, Adv. Chem. Phys. **70**, 53 (1987), and references therein.
[27] For details on how to obtain the RM/TST maximum-likelihood values of ν_{eff}, see R. Hernandez, Ph.D. thesis, University of California, Berkeley, 1993 (unpublished).
[28] J. L. Duncan and P. D. Mallinson, Chem. Phys. Lett. **23**, 597 (1973).
[29] D. E. Reisner, R. W. Field, J. L. Kinsey, and H. L. Dai, J. Chem. Phys. **80**, 5968 (1984).
[30] G. E. Scuseria and H. F. Schaefer, J. Chem. Phys. **90**, 3629 (1989).
[31] M. Dupuis, W. A. Lester, B. H. Lengsfield, and B. Liu, J. Chem. Phys. **79**, 6167 (1983).
[32] M. J. Frisch, J. S. Binkley, and H. F. Schaefer, J. Chem. Phys. **81**, 1882 (1984).